Electron paramagnetic resonance studies of Kevlar 49 fibres: Stress-induced free radicals

I. M. Brown and T. C. Sandreczki
McDonnell Douglas Research Laboratories, St. Louis, Missouri 63166, USA

and R. J. Morgan
Lawrence Livermore National Laboratory, Livermore, California 94550, USA
(Received 18 August 1983)

Electron paramagnetic resonance (e.p.r.) spectroscopy was used to investigate the free radicals that are created in Kevlar 49 fibres as the result of stress-induced macromolecular chain scissions. Background spectra in the untreated fibres indicate the presence of several transition metal ions and also several ($\geqslant 3$) different types of free radicals. Mn^{+2} ions were positively identified from the e.p.r. spectrum of frozen solutions of concentrated sulphuric acid containing Kevlar 49. The other paramagnetic transition metal ions present were Cu^{+2}, and possibly Fe^{+2}, Fe^{+3}, Cr^{+3}, and Ti^{+3}. The observed anisotropy in the e.p.r. lineshapes indicates that some of the complexed metal ions together with their first co-ordination spheres are oriented in the crystalline regions of the Kevlar 49 fibres. Stress-induced free radicals were observed in previously annealed samples of Kevlar 49 fibres that had been fractured in a vacuum. The concentration of stress-induced radicals (2×10^{10} per filament) suggests that chain scission occurs in more weak planes than are estimated to exist in the fracture surfaces of the fibre core. These radicals are unstable in air and have some aromatic character associated with their structure. The characteristics of the stress-induced radicals in Kevlar 49 and nylon-6 are compared and the results are related to the different fibre morphologies.

(Keywords: Kevlar 49 fibres; electron paramagnetic resonance; free radicals; fracture stress; chain scission)

INTRODUCTION

The commercial aramid fibre, Kevlar 49 [poly(*p*-phenylene terephthalamide, PPTA][1], is presently being used as a reinforcing fibre in fibrous epoxy composites. In many applications these composite materials are expected to function reliably over a period of several years. It is therefore important to identify the chemical and physical features that determine the deformation and failure modes of the fibre and also how these features are modified by different environmental exposures.

There is evidence from stress rupture tests conducted at the Lawrence Livermore National Laboratory[2] under fluorescent lighting that macromolecular chain scission occurs in Kevlar 49 fibres. Although it seems reasonable to assume that macromolecular chain scission can lead to reduced tensile and compressional strength of the fibre, details of its exact role in determining the mechanical properties are uncertain. Two possible causes of chain scission in Kevlar 49 fibres that involve free radical formation are[2] (1) long term tensile loading and (2) irradiation by ultraviolet (u.v.) light. In this paper we describe the results of electron paramagnetic resonance (e.p.r.) experiments which were designed to investigate the formation of stress-induced free radicals in Kevlar 49 fibres.

EXPERIMENTAL METHODS AND RESULTS

Experimental details

All experiments were performed with a commercial *X*-band spectrometer which employs homodyne detection and 100 kHz modulation (Varian Model E-112E). The e.p.r. spectra were stored on magnetic tape using a data acquisition system (Varian Model E-900). These spectra could be field-shifted, scaled, subtracted, added, and integrated using the available software. The signal averaging capability of the data acquisition system was particularly useful in this study. In some of the low-intensity e.p.r. spectra where signal/noise was a problem, signal accumulation times as long as ~ 6 h were used (i.e., 600 scans at 35 s/scan). Most of the measurements were made on samples wound from a spool of Kevlar 49 fibres which was obtained from the Lawrence Livermore National Laboratory, where it had been stored in the dark. However, the exact history of this spool with regard to its exposure to u.v. light, temperature variations, and humidity from the time of its manufacture by the E. I. duPont Chemical Company is unknown. The yarn on this spool was 380 denier consisting of ~ 267 filaments with a diameter of ~ 10 μm and a producers twist of ~ 3 turns/m.

Our initial experiments showed the presence of background EPR spectra in the as-received Kevlar 49. The lineshapes were found to depend on θ, the angle between the fibre axis and the direction of the applied Zeeman magnetic field H_0. The anisotropy in the spectral lineshapes was studied using the two types of sample geometries shown in *Figure 1a* and *1b*. The former consisted of typically 25 (or fewer) continuous loops, i.e., 50 strands or 13 000 filaments. This sample was pulled into a 5 mm quartz or Pyrex tube and was always

0032-3861/84/060759-07$03.00

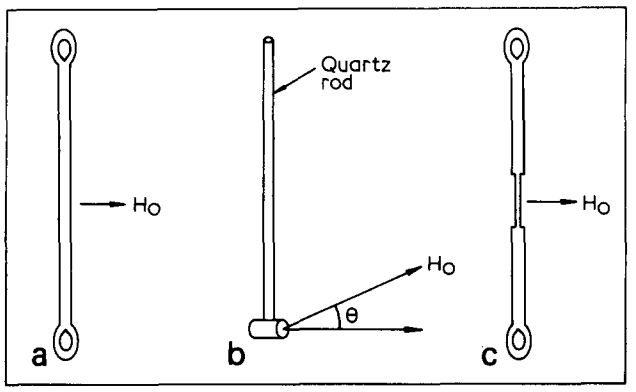

Figure 1 Geometries of Kevlar 49 fibre samples

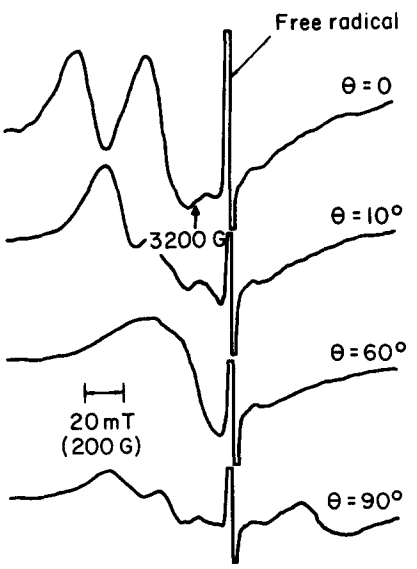

Figure 2 Transition metal ion spectra observed in oriented Kevlar 49 fibres at 295 K

mounted vertically in the microwave cavity so that $\theta = 90°$. The sample geometry shown in *Figure 1b* typically consisted of 50 strands, i.e., 13 000 filaments pulled through a 4 mm quartz tube and carefully cut at each end to give a sample length of 7 mm. This tube was slipped into a 5 mm quartz tube which had been fused to a 3 mm diameter quartz rod. The sample was then mounted with the quartz rod positioned vertically in the microwave cavity so that the sample could be rotated to allow all orientations of θ from 0 to 90°.

Background transition metal ions in Kevlar 49

The background spectra observed in the Kevlar 49 fibres could be classified into two categories: transition metal ion spectra or free radical spectra. It was usually clear from the linewidths and the anisotropy of the magnetic field values at which the lines occurred how the observed lines were to be assigned; for example, in the spectra shown in *Figure 2*, taken at the different values of θ shown, the free radical line can clearly be distinguished from the lines assigned to the transition metal ion(s). The anisotropy in the latter lines, because of either fine structure, hyperfine structure and/or g-anisotropy, is approximately 90 mT, whereas the g-anisotropy in the free radical line produces field shifts of only ~0.3 mT.

Identification of the transition metal ion(s) in Kevlar 49 fibres solely from the orientation dependence of the e.p.r. spectra is difficult. Although the metal ion complex is oriented with respect to the fibre axis, its orientation with respect to the other two axes perpendicular to the fibre axis, is random. Clarkson[3] has attributed these spectra to Cu^{+2}, but the following observations make this premise seem unlikely.

Estimates of the different metal contents in Kevlar 49 fibres have been made using atomic emission spectroscopy[4], atomic absorption spectroscopy[5], and spark source mass spectroscopy[4]. *Table 1* lists the metals that give rise to paramagnetic ions selected from all metals detected by these techniques together with their estimated concentrations. The metal impurities having the highest concentrations in the Kevlar 49 fibres need not necessarily show the most intense e.p.r. absorption lines if the associated linewidths are large. Moreover, the metal ions may be present in the Kevlar 49 fibres in a diamagnetic oxidation state, e.g., Ti^{+4}.

In a related experiment, samples of Kevlar 49 were dissolved in concentrated sulphuric acid. These samples were carefully prepared in a nitrogen-filled glove box to exclude moisture. No spectra could be detected in the Kevlar/sulphuric acid solution at 300 K, whereas the spectrum shown in *Figure 3* was obtained from a sample containing 10 wt% Kevlar in sulphuric acid frozen at 77 K. This spectrum consists of a single intense line at $g = 1.945$ and approximately 18 less intense lines with a magnetic field spread of 60 mT. The onset of liquid crystal domain ordering is supposed to occur at concentrations of 9 wt% Kevlar[6,7]. However, no essential difference between this spectrum and that observed from a sample containing 2.5 wt% could be detected.

Manganese (II) sulphate was dissolved in a small amount of water followed by the addition of concentrated sulphuric acid. This solution was diluted with concentrated sulphuric acid to form a solution containing >99% acid before transferring it to a sample tube. The spectrum at 77 K of a frozen sample of this solution is shown in *Figure 3* along with the spectrum of the frozen Kevlar 49/sulphuric acid sample. The former was appropriately scaled and subtracted from the latter to give the spectrum shown in *Figure 3c*. It is clear that 16 lines in the spectrum

Table 1 Trace metal content in Kevlar 49 fibres

Element	Spark source[a] mass spectroscopy (ppm)	Atomic emission[a] spectroscopy (ppm)	Atomic absorption[b] spectroscopy (ppm)
Fe	50	10	72
Ti	<20	6	1.3
Cu	<0.8	4	0.4
Cr	<0.7	2	42
Ni	<0.5	2	14
Mn	<0.5	0.2	1
Co	<0.5	<0.06	<0.5
Ag	–	<0.06	1.5
Ce	<1.0	<0.06	–
Nd	<5.0	–	–
Sm	<5.0	–	–
En	<2.0	–	–
Gd	<6.0	–	–
Ho	<1.0	–	–
Yb	<5.0	–	–
Dy	<5.0	–	–

[a] See Reference 4
[b] Measurements made at McDonnell Douglas Corporation

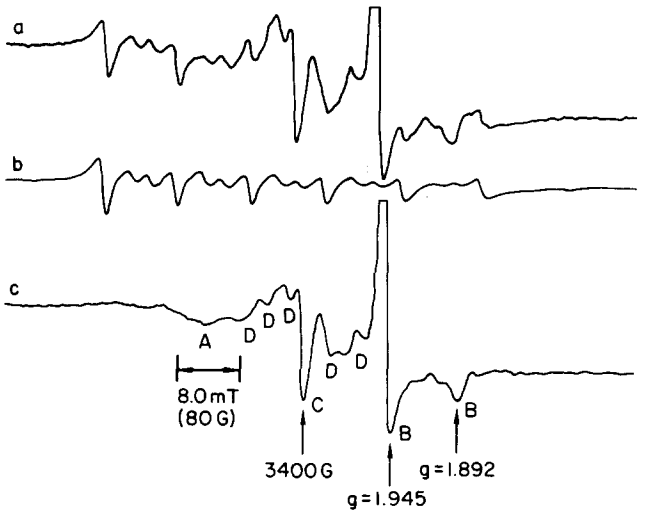

Figure 3 E.p.r. spectra obtained at 77 K from: (a) Kevlar 49 in concentrated sulphuric acid, (b) $MnSO_4$ in concentrated sulphuric acid, and (c) difference (i.e., spectrum (a) minus spectrum (b))

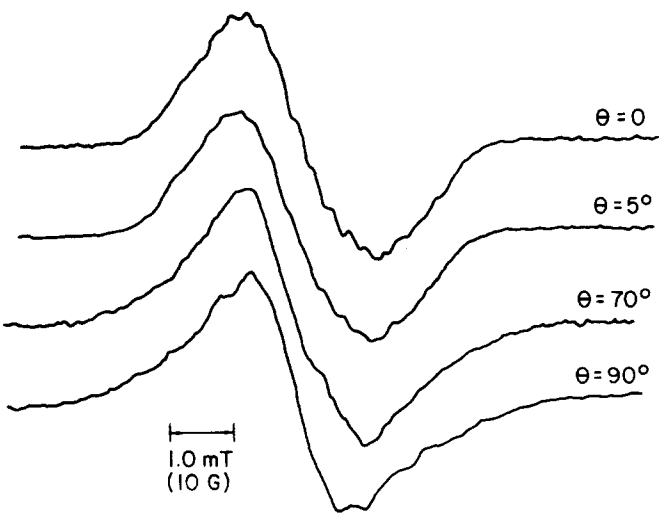

Figure 4 Background free-radical spectra in Kevlar 49 fibres at different values of θ

in *Figure 3b* correspond to the 6 allowed hyperfine transitions and 10 forbidden hyperfine transitions associated with the Mn^{+2} ion[8].

Samples of Fe^{+3}, Cu^{+2}, Cr^{+3}, and Ti^{+3} in concentrated sulphuric acid were also prepared by dissolving the appropriate salt in the acid. These samples show that Fe^{+3} and Cr^{+3} exhibit broad lines (linewidths $\gg 50$ mT) at 77 K which could not be identified with any of the lines in *Figure 3c*. However, because of the high iron and chromium contents in Kevlar 49 (see *Table 1*), we can reasonably expect Fe^{+2}, Fe^{+3} and Cr^{+3} to be present in the Kevlar 49 sulphuric acid dopes and also in the Kevlar 49 fibres. The line A occurs at the same field as the main line in the Cu^{+2} spectrum. The low intensity of the line A in *Figure 3c* indicates the low relative importance of Cu^{+2} as a paramagnetic transition metal impurity in Kevlar 49. The line B can be assigned to a metal ion with an axially symmetric g tensor. The values of $g_{\parallel} = 1.945$ and $g_{\perp} = 1.892$ could correspond to those expected from the Ti^{+3} ion[9]. The lines C and D are as yet unidentified.

It has not yet been established which transition metal ions are responsible for the anisotropic spectrum shown in *Figure 2*. However, the observed anisotropy indicates that these transition metal ions together with their first coordination spheres are oriented in the crystalline regions of the Kevlar 49 fibres.

Background free radicals in Kevlar 49

Contrary to other results reported in the literature[3], we have found that the e.p.r. lineshape for the background free radicals in Kevlar 49 fibres is anisotropic. The spectra obtained at different orientations of the fibre axis to the magnetic field direction are shown in *Figure 4*. The best resolution of the hyperfine structure was obtained at $\theta = 0$. This behaviour implies that some (or all) of these background free radicals are oriented in the crystalline lattice of the Kevlar 49.

In the initial attempts to detect stress-induced free radicals, it was clear that the background free radical e.p.r. spectra were large enough to limit the level of detectibility. Kevlar 49 samples were annealed in a nitrogen atmosphere at 453 K, 523 K and 573 K for approximately 15 h before the spectra were recorded at 293 K. After each annealing period, the spectra showed a reduction in the integrated intensity and a change in the lineshape. *Figure 5* shows the lineshapes before annealing and after 15 h annealing at 453 K and 523 K respectively. The spectra were manipulated with the available software in the data acquisition system. Appropriately scaled spectra were subtracted from one another to give the spectra of the free radical species that decomposed at 453 K, 523 K, and 573 K. These spectra are shown in *Figures 6b–6d*, respectively.

Stress-induced free radicals in Kevlar 49

Initial experiments were performed by stressing samples consisting of several strands ($\sim 20\,000$ filaments) of Kevlar 49 fibres in air at room temperature with a stress testing instrument (Instron model 1102) outside the e.p.r. cavity. Various load stresses were applied up to and including fracture. In none of the stressed samples, including the ruptured strands, were e.p.r. spectra observed that could be assigned to stress-induced free radicals. All samples showed the typical background e.p.r. spectra.

An aluminum frame was constructed for installation directly in the magnetic field gap to allow the Kevlar 49

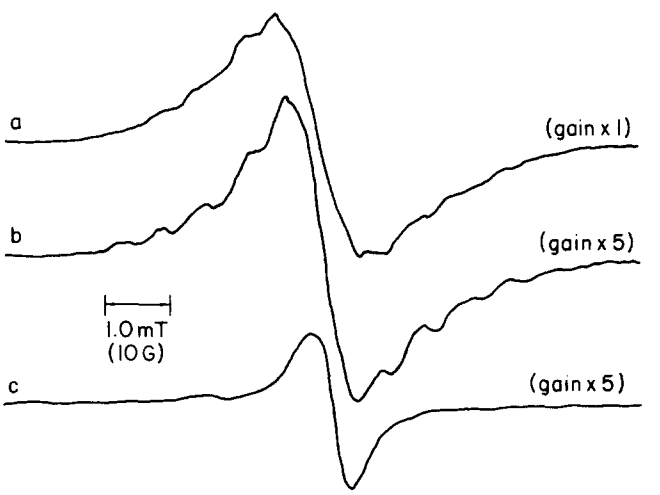

Figure 5 E.p.r. spectra observed in Kevlar 49 fibres at 295 K with $\theta = 90°$ after (a) no heat treatment, (b) heating at 453 K in nitrogen for 15 h, and (c) heating at 523 K in nitrogen for 15 h

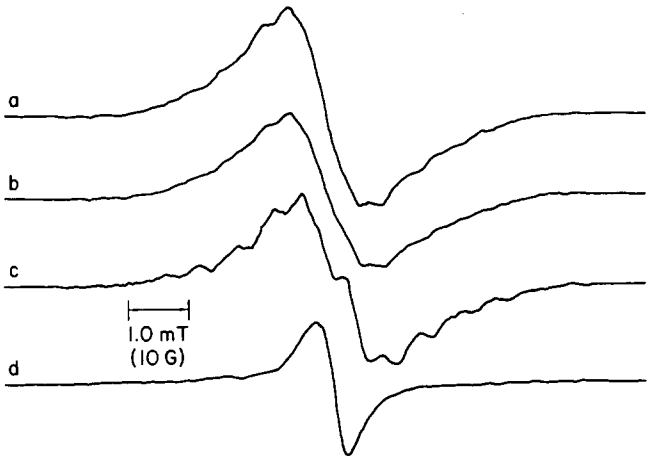

Figure 6 E.p.r. spectra observed in Kevlar 49 fibres at 295 K with $\theta = 90°$; (a) background spectrum; (b) spectrum (a) minus 0.2 × spectrum shown in *Figure 5b;* (c) spectrum in file 1 minus spectrum in file 2; (d) spectrum in file 2 recorded after heating at 523 K for 15 h

fibres to be stressed in the cavity. The fibres were epoxied between plastic grips (25 × 75 × 17 mm) which were held with stainless steel grips. The fibres were stressed vertically in the cavity while exposed to air. No stress-induced radicals could be detected in these experiments. The background signal was observed in all samples and showed no detectable reduction in intensity following application of stress.

Work reported in the literature[10-13] suggests that most types of stress-induced radicals react quickly with atmospheric oxygen. We therefore modified the stress rig to allow the Kevlar 49 fibres to be stressed in a vacuum or an inert atmosphere inside the microwave cavity. The modified form of the rig is shown in *Figure 7*. The fibres were stretched vertically inside an 11 mm o.d., 9 mm i.d. quartz tube which was mounted vertically in the cavity. A Cajon fitting containing an O-ring vacuum seal at either end of the quartz tube allowed the vacuum to be maintained around the fibres. Each end of the looped fibres was held over a bushing (4 mm o.d.) and pin (3 mm o.d.) positioned at the end of a stainless steel rod (6 mm o.d.). Each of these rods could be moved through an additional Cajon fitting containing an O-ring vacuum seal. The tensile loading levels were measured with a load cell (Interface Model SM-1000).

The samples consisted of 60 strands (i.e., 30 loops) of Kevlar 49 fibres which, except for the end loops and a region 10 mm either side of centre, were coated with a quick setting epoxy regin. After removal of ~40 strands located 10 mm on either side of centre, the remaining fibres were also coated with a quick-setting epoxy resin. This sample geometry ensured that the strands always fractured at the centre of the loops inside the microwave cavity. Several samples with this geometry were stressed up to fracture in a vacuum in the cavity. No e.p.r. spectra associated with free radicals generated by stress-induced bond scissions could be identified. It was clear that the detection limit of the stress-induced radicals was set by the background spectrum. It was estimated that this limit was ~2% of the background intensity. A series of experiments was therefore performed to investigate how the concentration of background free radicals could be reduced by annealing the fibres in a nitrogen atmosphere. The results have been described above but the main quantitative result is that after heating the Kevlar 49 fibres in nitrogen at 523 K for 15 h, the background integrated e.p.r. spectrum intensity was reduced to ~17% of the value observed in the unannealed sample. The stress–e.p.r. experiments were then repeated on these annealed samples in a vacuum. The sample geometry was the same as that described above and is shown in *Figure 1c*.

The e.p.r. signal was monitored at each setting of the applied stress. No e.p.r. spectra associated with stress-induced radicals were observed below fracture. Moreover, no reduction in the background signal could be detected (sensitivity was ~2% of the background intensity) below fracture. Following fracture, however, an e.p.r. line was observed superimposed on the remnant background spectrum. In these experiments the sample was degassed at a high vacuum (~1 mPa) for at least 15 h. The e.p.r. spectrum of the stress-induced radicals created after fracture was then usually stable without any observable reduction in intensity for 6 or 7 h. However, in a sample which had been degassed for only ~2 h, measurable decay in the spectrum of the stress-induced radicals could be detected after ~2 h. The latter result is shown in *Figure 8*. When air was admitted to all fractured samples, the spectrum associated with the stress-induced signal instantly disappeared. On the subsequent return of a vacuum to the quartz tube, the stress-induced signal did not reappear, and only the background signal remained.

It was possible to manipulate the stainless steel rods while the fractured sample was inside the evacuated quartz tube without breaking the vacuum. Thus, the rods could be withdrawn so that the fracture surfaces were removed from the cavity. In this way it could be demonstrated that the stress-induced radicals were located only within a few millimetres of the fracture surfaces. This result explains why no stress-induced radicals were obser-

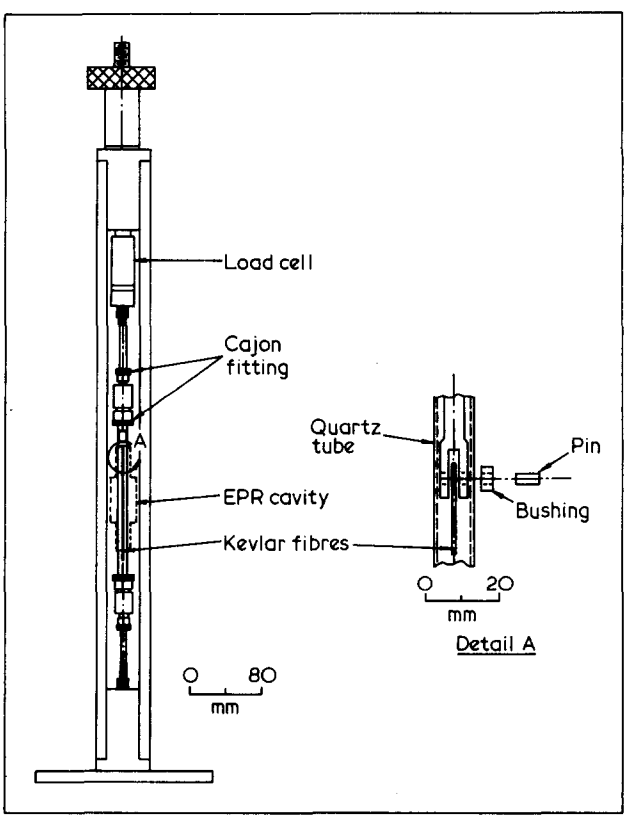

Figure 7 Experimental arrangement for stressing Kevlar 49 fibres in a vacuum

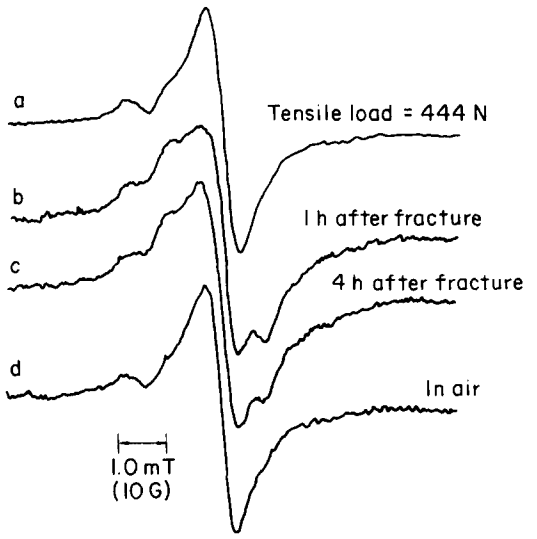

Figure 8 E.p.r. spectra observed in Kevlar 49 fibres with $\theta = 90°$ in applied stress experiments (a) after annealing at 523 K for 15 h with applied tensile load = 444 N, (b) 1 h after fracture in a vacuum, (c) 4 h after fracture in a vacuum, and (d) after exposure to air

ved in samples where fracture occurred outside the cavity. Secondly, rotating the rods and hence also the fracture ends resulted in no change in the stress-induced radical e.p.r. signal. The latter result suggests that there is little anisotropy associated with the stress-induced radicals, i.e., they are randomly oriented. This observation, along with the fact that the stress-induced spectrum disappears on exposure to air, eliminates the possibility that the e.p.r. signal appearing after fracture is the results of any anisotropy in the background signal.

The radical concentrations were estimated by subtracting an appropriately scaled version of the background spectrum from the spectrum observed after fracture. The scaling procedure, however, is somewhat arbitrary. The difficulty arises because the sample filling factor (and hence the gain of the spectrometer) is different before and after fracture. In many cases, at fracture, one end of the fractured fibres was ejected from the cavity. These fibres could always be reinserted into the cavity without breaking the vacuum using the steel rod, but even then it was not clear how the filling factor compared with that before fracture. As a consequence, the exact shape of the spectrum associated with the stress-induced radicals could not be positively identified, and the area under this spectrum could not be accurately determined.

Figures 9 and *10* illustrate the typical spectral subtraction procedure. In *Figure 9* the spectrum before and after fracture has been normalized by multiplicative software to the same peak height. Subtraction of these spectra result in the doublet spectrum shown in *Figure 9b*. On the other hand, if the background spectrum is scaled down by a scale factor $\gtrsim 0.5$, the resulting difference spectrum clearly shows the presence of a remnant background spectrum. The best fit to a single-line spectrum is given by the scaling factor 0.8 and is shown in *Figure 9c*. We estimate that the uncertainty in choosing this scaling factor correctly produces an error of $\pm 20\%$ in the estimates for the radical concentration.

The stress-induced radical concentration is determined from a double integration of the lineshape in *Figure 9c* using the available software. A typical example is shown in *Figure 10*. The spectrum of a standard sample is then recorded with the same spectrometer gain settings and also double integrated. Two standard samples were prepared from a Varian strong pitch[14] sample by further dilution with potassium chloride. The spin concentrations of these standard samples were 4.4×10^{13} and 4.6×10^{14} spins/cm. We assumed the same filling factors for the Kevlar 49 fibres and the standard samples, i.e., both are line samples with approximately the same diameter (~ 4 mm). Our estimate of the number of free radicals produced in each 10 μm diameter Kevlar 49 filament as a result of stress-induced bond scissions is $2 \times 10^{10} \pm 20\%$.

Nylon-6 (polycaprolactam) fibers have been reported to exhibit large concentrations of stress-induced radicals[10-13]. We also investigated nylon-6 fibres both to determine the sensitivity and capability of detecting stress-induced radicals with our equipment and also to compare the characteristics of the stress-induced radicals in Kevlar 49 fibres with those in nylon-6.

A bundle of nylon-6 fibres was stressed in vacuum inside the microwave cavity. The results in nylon-6 show the following characteristics, some of which have been

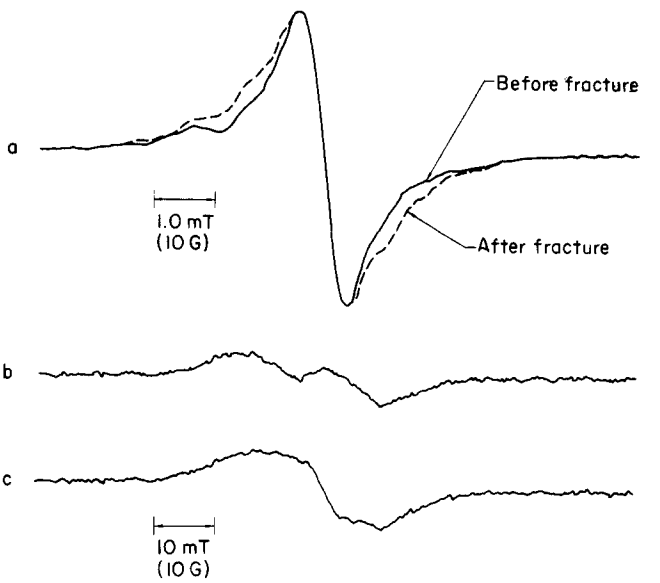

Figure 9 (a) E.p.r. spectra observed in Kevlar 49 fibres with $\theta = 90°$ before and after fracture in a vacuum. E.p.r. lineshapes associated with stress-induced free radicals; (b) spectrum after fracture minus the background spectrum, and (c) spectrum after fracture minus 0.8x (background spectrum)

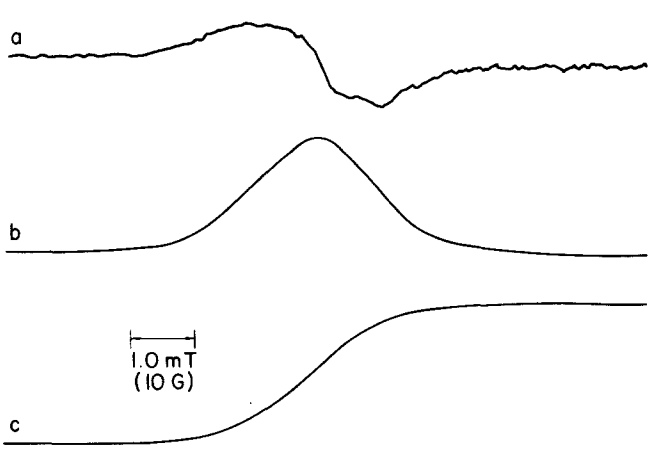

Figure 10 Typical (a) derivative spectrum, (b) absorption spectrum, and (c) integrated absorption spectrum

described[10-13]: (1) There was a background signal present in our sample of nylon-6. (2) Free radicals are formed in nylon-6 as a result of bond scissions induced by applied stress. The amount of these free radicals is one to two orders of magnitude larger than that of the stress-induced radicals in Kevlar 49 fibres. (3) These stress-induced radicals can be detected at stresses well below the value required to cause fracture. (4) At low tensile loads, the lineshapes show that the background signal is not present. This result would indicate that the background radical has decayed as a result of the applied stress. Hence, the background radicals have reacted with some of the stress-induced radicals. (5) When the applied stress was removed, there was no measurable decrease in the radical concentration. (6) When the stress was reapplied, the radical concentration increased only when the strain level was increased beyond the largest value reached before the removal of the stress. (7) There was no great increase in radical formation from just before to just after fracture. (8) When air was admitted to the sample, the spectrum associated with the stress-induced radicals instantly disappeared.

DISCUSSION

Kevlar 49 fibres consist of extended-chain, rod-like macromolecules of PPTA aligned along the fibre direction[2,16]. Electron diffraction and electron microscope dark-field image studies of Kevlar 49 fibres by Dobbs *et al.*[17] have revealed Kevlar 49 fibres can consist of a system of H-bonded sheets regularly pleated along their long axes and arranged radially. This supermolecular structure leads to periodic bands of strained macromolecules along the fibre axis with a spacing of 250 and 500 nm. This spacing has been associated with the pleat structure periodicity[16,17]. However, Morgan *et al.*[2,18] while not disputing the evidence for the pleat morphology of Kevlar 49 fibres suggest the primary structural factors affecting the deformation and failure processes and strength of Kevlar 49 fibres, are the concentration and distribution of the macromolecular chain ends within the fibres. Based on the fibre fabrication procedures (the physical processes involved upon Kevlar 49/H_2SO_4 doped crystallization), and the fibre deformation and failure processes) they proposed the model illustrated in *Figure 11b* of the chain end distribution in Kevlar 49 fibres. The fibre consists of a 0.1 to 1.0 μm thick skin surrounding a core region which contains bundles of 60 nm diameter cylindrical crystallites oriented in the direction of the fibre axis. In the skin region the chain ends are randomly distributed, whereas in the interior core region there is a clustering of the chain ends so that periodic transverse weak planes are separated by a distance of $\sim$220 nm. Fracture topography studies of Kevlar 49/epoxy composites and bare yarns indicate both the weak planes and the 60 nm granular morphology shown in *Figure 11b*.[2] These weak planes are depicted in *Figure 11* as gaps between the crystallites, but they should be considered as planes of maximum chain-end concentrations since a large percentage of macromolecular extended chains still traverse the planes. In this way structural continuity and integrity are maintained.

The nonuniform distribution of chain ends may be caused by the tendency of ionic end groups to cluster at some stage in the fibre fabrication process[2,18]. Thus, the clustering may occur in the liquid crystalline domains that occur in the PPTA/sulphuric acid dopes and/or during crystallization after exiting from the spinneret in the fibre spinning process.

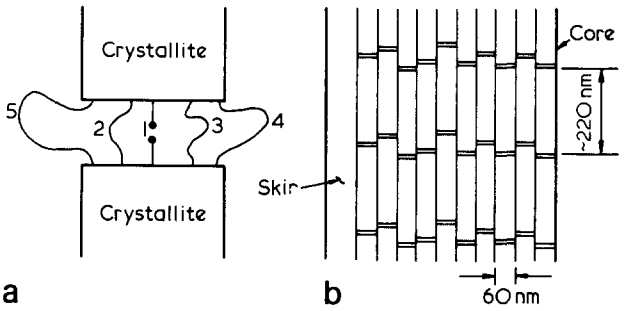

Figure 11 Models for the morphologies in (a) nylon-6 and (b) Kevlar 49

The known differences in the morphologies of the nylon-6[10] and Kevlar 49 fibres[2] can explain the differences in the behaviour of the stress-induced radicals in these polymers. The Peterlin model[10] for the nylons is shown in *Figure 11a*. The crystalline regions contain folded chains but in such a way that the same chain can be located in different crystallites. The sections of the chains that traverse the amorphous regions between the crystallites can be considered as tie molecules which are held firmly at either end in the crystallites. Since there will be a distribution in the lengths of the tie molecules, an applied stress will result in a stress concentration on the shortest tie molecules. As the applied stress is increased, chain scission will occur progressively when each tie molecule in sequence is strained beyond its maximum length. Thus, in the example in *Figure 11a*, chain scission will occur in the numerical order shown. Stress-induced free radicals are therefore observed at stress levels well below that required for filament fracture. Moreover, the concentration of radicals observed depends on the strain levels attained.

The situation is different in Kevlar 49 because of the highly extended-chain, rod-like nature of the PPTA molecules. Here the chains traversing the weak planes can constitute the tie molecules. For a given applied stress, there should be a more uniform distribution of molecular stress and strain over the tie molecules. All chain scissions are supported by the observation of stress-induced free radicals which occur over a narrow distribution of strain levels, i.e., at fracture. Although stress-induced radicals were not detected in these experiments at stress levels below fracture, the possibility that some chain scission has occurred should not be neglected. Rather, it should be concluded that if chain scission has occurred the few free radicals produced are below the detectable limit. This result implies that the amount of chain scission below fracture is less than $\sim 1/20$ of that observed after fracture (i.e., $< 10^9$ chain scissions per filament).

The e.p.r. results on nylon-6 indicated that the background radicals reacted with the stress-induced radicals to remove the background spectrum at low strain values. However, after fracture of the Kevlar 49 fibres, the stress-induced radicals were observed in the presence of a much larger background spectrum (the integrated intensities differed by a factor of 4). Thus, there was no indication of reaction between the background radicals and the stress-induced radicals which were observed after

fracture. It therefore appears likely that if stress-induced radicals are created before fracture, they do not react with the background radicals.

The tendency of chains to slip past one another can lead to chain pull-out from the cylindrical crystallites. This chain pull-out will compete with chain scission in the failure modes of the Kevlar 49 fibre. The smaller number of stress-induced radicals observed in Kevlar 49 as compared with nylon-6 may be the result of chain-scission processes competing less favourably with chain pull-out in the Kevlar 49 fibres.

The number of chains in a fibre filament cross section was calculated from the known unit cell dimensions[19] ($0.787 \times 0.512 \times 1.29$ nm). Assuming one chain occupying the area of a unit cell cross section (0.41 $(nm)^2$), the number of chains in a single filament cross section is 2×10^8. If all these chains undergo scission, the maximum number of primary free radicals to be expected is 4×10^8 per filament. Our estimate of the number of stress-induced radicals after fracture is 2×10^{10} radicals per filament with an accuracy of $\pm 20\%$. It is assumed that the stress-induced radicals, which are probably secondary radicals, are not produced in a larger concentration than the primary radicals created in the initial chain scission process. The discrepancy between the observed value and the maximum estimate could imply that chain scission occurred at 50 times as many weak planes as are associated with one transverse fracture plane, which is approximately equivalent to all chains within the weak planes undergoing scission over a longitudinal distance of $(50 \times 200\ nm) = 10\ \mu m$ or $5\ \mu m$ distance from each fracture surface. In reality bundles of unimpregnated Kevlar 49 filaments or filaments in epoxy composites fail in tension, by axially splitting over distances of 250–500 μm along their lengths[2,18,20]. This implies that for a filament that failed by axially splitting 500 μm, only 2% (=10/500) of the chains that pass through each transverse periodic weak plane have undergone scission.

In nylon-6 the stress-induced radicals have been identified with secondary main-chain radicals that are formed as the result of a hydrogen atom abstraction from nearby chains by the primary radicals created in the initial chain scission event[10,11,13]. The stress-induced radicals in Kevlar 49 are probably also secondary radicals. The linewidths of these radicals in Kevlar 49 (~1.0 mT) are observably smaller than the overall linewidth of the radicals in nylon-6 (~12 mT). This result may indicate that the radical structure in Kevlar 49 has more electron delocalization and hence more aromatic character than the radical structures in nylon-6.

Instead of tensile-induced macromolecular chain scission it cannot be discounted that the radicals produced upon fibre fracture result from chain scission within the kink-band deformation zones that form in compression as the fractured fibre ends snap back[2,21]. The inability of the rigid, extended-chain macromolecules to accommodate *c*-axis rotations of up to 67° upon compression-induced kink-band deformation would lead to chain scission in the region of the propagating kink[20].

ACKNOWLEDGEMENT

This research was performed under the University of California, Lawrence Livermore National Laboratory Purchase Order 3115901.

REFERENCES

1 Manufactured by E. I. duPont Chemical Company, Wilmington, Delaware
2 Morgan, R. J., Pruneda, C. O., and Steele, W. J. *J. Polym. Sci., in press*
3 Clarkson, R. B., 'Molecular Motion in Polymers by ESR' (Eds R. F. Boyer and S. E. Keinath), Michigan Molecular Institute Press, Midland, Michigan, 1980
4 Penn, L. and Larsen, F. *J. Appl. Polym. Sci.* 1979, **23**, 59
5 McDonnell Douglas Corporation unpublished data
6 Kwolek, S. W., E. I. duPont, U.S. Patent 3,671,542, 1972
7 Onogi, Y., White, J. L. and Fellers, J. F. *J. Polym. Sci.* Polym. *Phys. Edn.* 1980, **18**, 663
8 Bleaney, B. and Rubens, R. S. *Proc. Phys. Soc.* 1961, 77, 103
9 Chester, P. F. *J. Appl. Phys.* 1961, **32**, 2233
10 Peterlin, A. *Polym. Sci.* 1970, **C32**, 297
11 Kausch, H. H. 'Polymer Fracture' (Springer Verlag, New York, 1978)
12 Nagamura, T. and Takayanagi, M. *J. Polym. Sci.* 1974, **12**, 2019
13 Backman, D. K. and DeVries, K. L. *J. Polymer Sci. A-1* 1969, **7**, 2125
14 The Varian strong pitch sample contains 2.5×10^{15} spins/cm, whereas the Varian weak pitch sample contains 1.0×10^{13} spins/cm
15 Dobb, M. G., Johnson, D. J. and Saville, B. P. *Phil. Trans Roy. Soc. London* 1980, **A294**, 473
16 Avakian, P., Blume, R. C., Gierke, T. D., Yang, H. H. and Panar, M. *Polym. Prepr.* 1980, **21**, (1) 8
17 Dobb, M. G., Johnson, D. J. and Saville, B. P. *J. Polym. Sci. Polym. Phys. Edn.* 1977, **15**, 2201
18 Pruneda, C. O., Steel, W. J., Kershaw, R. P. and Morgan, R. J. *Polym. Prepr.* 1981, **22**, 217
19 Northolt, M. G. and van Aartsen, J. J. *J. Polym. Sci. Polym. Phys., Edn.* 1973, **11**, 333
20 Morgan, R. J., Mones, E. T., Steele, W. J. and Deutscher, S. B. *Polym. Prepr.* 1980, **21**, 264
21 Konopasek, L. and Hearle, J. W. S. *J. Appl. Polym. Sci.* 1977, **21**, 2791